Appl. Phys. B 65, 151–159 (1997)

Applied Physics B Lasers and Optics

Invited paper

High-power sub-10-fs Ti:sapphire oscillators

L. Xu[1], G. Tempea[1], A. Poppe[1], M. Lenzner[1], Ch. Spielmann[1], F. Krausz[1], A. Stingl[2], K. Ferencz[3]

[1] Abteilung Quantenelektronik und Lasertechnik, Technische Universität Wien, Gusshausstr. 27, A-1040 Wien, Austria
(Fax: +43 1 504-2477, E-mail: krausz@ps1.iaee.tuwien.ac.at)
[2] FemtoLasers GmbH, Kleinenegersdorferstr. 24, A-2100 Korneuburg, Austria
[3] Research Institute for Solid State Physics of the Hungarian Academy of Sciences, P.O. Box 49, H-1525 Budapest, Hungary

Received: 10 March 1997/Revised version: 16 April 1997

Abstract. The state of the art of mirror-dispersion-controlled (MDC) Ti:sapphire laser oscillators is reviewed. Owing to improvements in the cavity and mirror design, these systems can now routinely generate sub-10-fs pulses with peak powers exceeding the megawatt level. The unique compactness of MDC Ti:sapphire oscillators results in excellent noise characteristics, a nearly diffraction limited output, and a high reproducibility of performance. Employing a diode-pumped solid-state laser as a pump source allows the generation of sub-10-fs pulses from an all-solid-state laser for the first time.

PACS: 42.55.Rz; 42.60.Mi; 42.65.Re

Titanium-doped sapphire lasers [1] generating ultrashort pulses by Kerr-lens mode locking (KLM) [2–7] are now widely used for time-resolved studies in physics, chemistry, biology, and electronics, as well as for seeding high-power solid-state amplifier systems. After its first demonstration by Spence and co-workers in 1990 [2], the performance of KLM Ti:sapphire oscillators had been subject to a rapid progress [8], which temporarily culminated in the development of fused-silica-prism-controlled systems [9]. When detuned to ≈ 850 nm, these systems have been capable of generating pulses of around 10 fs or slightly shorter in duration [10, 11], which were limited by the fourth-order dispersion introduced by the prisms [12]. This performance came at the expense of a large (> 0.6) time–bandwidth product and a significant red shift of the spectrum from the gain peak of Ti:sapphire, impairing the suitability of this broadband output for seeding Ti:S amplifiers.

With the advent of dispersion-engineered chirped multilayer dielectric mirrors [13] a new generation of mirror-dispersion-controlled (MDC) Ti:sapphire lasers has been developed [14–17] which were able to overcome the limitations inherent in prism-controlled oscillators. In MDC oscillators the mirrors not only provide feedback but also introduce broadband negative dispersion indispensable for soliton-like pulse formation [18]. Hence they obviate the need for intracavity prisms, allowing the construction of femtosecond Ti:S oscillators containing no intracavity components other than the gain medium (and an optional aperture). This unprecedented simplicity and compactness come in combination with a reliable sub-10-fs performance in the 800-nm wavelength range. Owing to these unique features, sub-10-fs MDC Ti:sapphire oscillators are likely to become an important workhorse for a number of application fields, particularly where high time resolution, high peak power, solid-state ruggedness, and reliability are important.

In this paper, we shall report on recent progress in MDC Ti:S oscillator technology, which has permitted the generation of femtosecond pulses with peak powers exceeding 1 MW for the first time directly from a laser oscillator. As this output is delivered in a nearly diffraction-limited beam, these sub-10-fs pulses are expected to be focusable to intensities well beyond the terawatt/cm^2 level. This performance is unprecedented in a cw mode-locked laser. Yet higher peak powers can be achieved by cavity dumping [19, 20] or external amplification [21] at reduced repetition rates.

The advanced sub-10-fs oscillator technology is the result of recent innovations in the design and optimization of KLM oscillators as well as of progress in chirped mirrors technology [22]. In what follows we shall focus on the laser design; details about the chirped mirror characteristics will be published elsewhere. After considering some general guidelines for optimizing KLM oscillators for maximum output pulse energy, the results of the optimization of MDC oscillators Kerr-lens mode-locked by using hard and soft apertures will be presented. The pulses delivered by the oscillators have been characterized temporally, spectrally, spatially (beam profile, M^2), as well as in terms of their energy noise and timing jitter. Finally, the major characteristics of an all-solid-state sub-10-fs laser will be briefly summarized.

1 Design considerations for high-power KLM oscillators

In femtosecond solid-state lasers a soliton-like interplay between self-phase modulation (SPM) and negative group delay dispersion (GDD) dominates the formation of an ultrashort pulse in the laser cavity. The separated action of SPM and GDD introduces a periodic perturbation to the soliton-like

mode-locked pulse upon circulation in the cavity. This periodic perturbation makes the pulse shed radiation to the continuum, i.e. to a cw background radiation which coexists with the mode-locked pulse [10, 23–26]. This undesirable energy flow from the mode-locked pulse to a cw background, which is intensified by the presence of high-order cavity dispersion [25], tends to increase with increasing Kerr-induced nonlinear phase shift per round-trip and give rise to instabilities. The maximum energy loss rate that can be tolerated depends on the strength of self-amplitude modulation (SAM, introduced by the fast saturable absorber-like action of KLM), which tends to suppress the low-intensity background, giving rise to a reverse energy flow [25]. From these considerations it is clear that increasing the intracavity pulse energy and/or decreasing the pulse duration call for (i) increasing the cross-sectional area of the resonator mode in the Kerr medium and/or (ii) improving the efficiency of the SAM action, if stable mode locking is to be sustained. Once the intracavity pulse energy is maximized, the output pulse energy can be increased by (iii) increasing the output coupling.

It is apparent that these measures can not be taken without trade-offs. For instance, requirements (i) and (ii) are contradictory, because an increased beam cross-section reduces the intensity in the Kerr medium and thereby the efficiency of SAM. Also, higher output coupling enhances gain guiding, which, again, reduces the modulation depth of SAM arising from an interplay between self-focusing in the gain medium and an intracavity aperture. Further, both (i) and (iii) tend to increase the (cw) laser oscillation threshold and hence compromise the overall efficiency. As a consequence, when optimizing a KLM Ti:S oscillator for maximum (output) pulse energy and minimum pulse duration, several parameters have to be mutually traded off against each other. In the following sections we shall present the results of this optimization procedure. Both hard and soft aperture have been used for mode locking.

2 Optimized hard-aperture and soft-aperture KLM Ti:S oscillators

The generic cavity configuration of the KLM Ti:S lasers used in our experiments is shown schematically in Fig. 1. The focusing elements, which are curved mirrors in practice, provide a tightly focused resonator mode in the gain medium if $d_1/f_1 \gg 1$ and/or $d_2/f_2 \gg 1$ is satisfied. A small beam diameter in the laser medium is desirable for both a low pump threshold for laser oscillation and a high intensity needed for efficient self-focusing for the KLM action. In order that such a four-mirror cavity can support a stable TEM_{00} Gaussian mode, the separation of the focusing elements d_f must be close to and somewhat larger than $f_1 + f_2$ [27]. Therefore it is convenient to define a stability parameter δ using the relation $d_f = f_1 + f_2 + \delta$. The range of values for which the resonator is stable is given by

$$0 < \delta < \delta_1 \qquad \text{and} \qquad \delta_2 < \delta < \delta_{\max}\,, \tag{1}$$

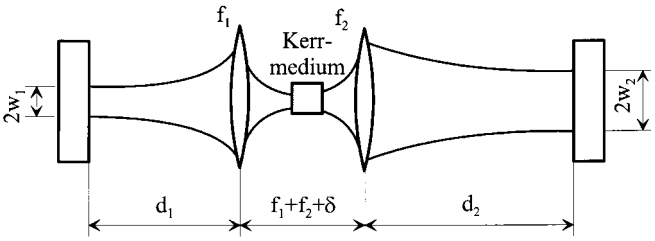

Fig. 1. Schematic diagram of the tightly-focused four-mirror resonator configuration used in the experiments

where

$$\delta_1 = \frac{f_2^2}{d_2 - f_2}, \qquad \delta_2 = \frac{f_1^2}{d_1 - f_1}\,, \quad \text{and} \qquad \delta_{\max} = \delta_1 + \delta_2\,. \tag{2}$$

Without loss of generality we have assumed $\delta_2 \geq \delta_1$. Figure 2 shows the $1/e^2$ beam diameter 2w, where w is the spot size of the Gaussian beam [28], at the ends of the laser cavity as a function of δ for the cavity parameters used in the experiments. Figure 2 reflects a general feature of the cavity schematically shown in Fig. 1; the stability range is subdivided in two distinct zones separated by a "forbidden" zone. The width of the latter increases with the cavity asymmetry parameter $\gamma = \delta_2/\delta_1 (\geq 1)$ [10]. The unstable zone disappears for an effectively symmetric cavity characterized by $\gamma = 1$.

Self-focusing introduced by the optical Kerr effect in the gain medium changes the confocal parameter of the cavity mode. Under specific conditions this change can result in better overlap with the pumped volume (soft aperture) or an increased transmittivity through a suitably positioned intracavity aperture (hard aperture). Both effects introduce a fast-saturable-absorber-like modulation, which can be approximately accounted for by an effective change in the round-trip gain as given by

$$\Delta g(t) = \kappa P(t)\,, \tag{3}$$

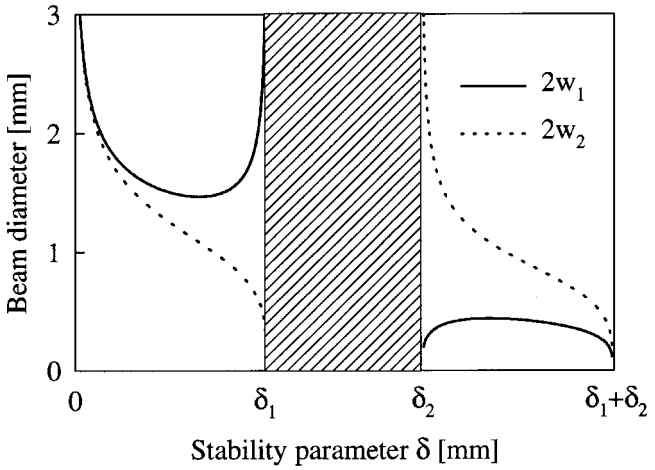

Fig. 2. Beam diameter at the cavity ends (see Fig. 1) as a function of the stability parameter δ for the cavity parameters $f_1 = f_2 = 5$ cm, $d_1 = 68$ cm, and $d_2 = 118$ cm

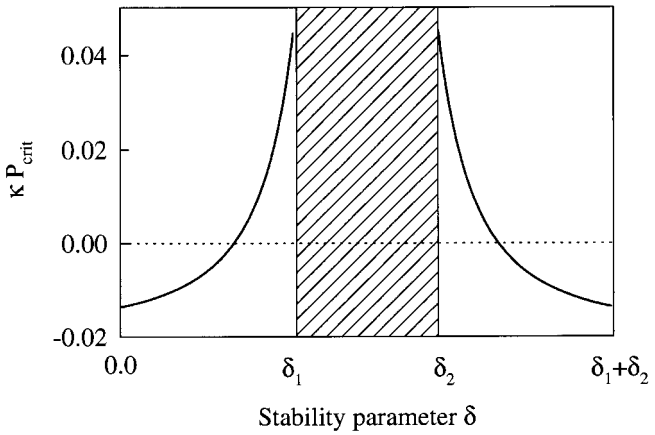

Fig. 3. SAM-coefficient κ for hard-aperture KLM (Eq. (3)) normalized to the critical intensity for self focusing in sapphire $P_{\text{crit}} = 2.6\,\text{MW}$ as a function of δ for the cavity parameters listed in the caption of Fig. 2. The sapphire Kerr-medium with a refractive index of 1.6 has a length of 2.3 mm. The circular aperture is inserted at the end of the shorter collimated arm and introduces a small-signal loss of 0.1. The resonator was assumed to have a cylindrical symmetry in the calculations

unless the instantaneous circulating power $P(t)$ approaches the critical power for self-focusing P_{crit} [29], which was evaluated as $P_{\text{crit}} \approx 2.6\,\text{MW}$ for sapphire [30].

Figure 3 depicts the SAM-parameter κ for hard-aperture KLM as a function of δ throughout the stability range for the case of a circular aperture being inserted in close proximity to the end of the shorter collimated cavity arm. Figure 4 shows κ as a function of δ, for two different values of the cavity asymmetry parameter. A nearly symmetric resonator ($\gamma \to 1$) permits a higher value of κ, which may allow even self-starting operation [31], but the condition $\kappa > 0$ requires operation closer to the boundary of the stability zone at δ_1. Experimentally, we have found $1.5 < \gamma < 2$ to be a good trade-off between efficient SAM and good stability against environmental perturbations for hard-aperture mode locking.

For soft-aperture KLM, an asymmetric cavity configuration was predicted to be most favorable for a strong SAM, provided that δ was adjusted close to δ_2 in the second stability

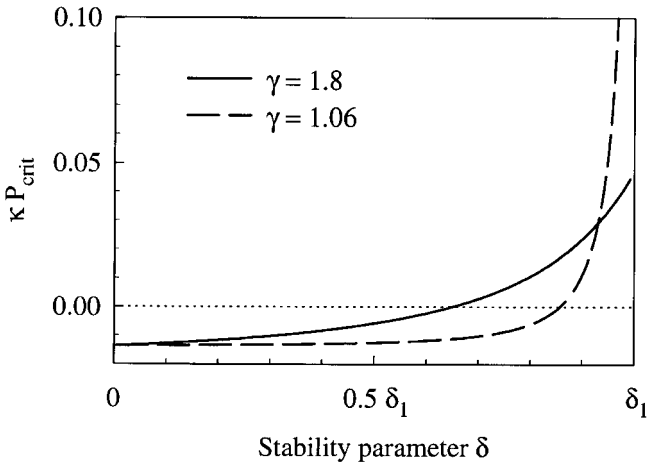

Fig. 4. The same as in Fig. 3 shown in the first stability zone for the laser parameters listed in the captions of Figs. 2 and 3 (*solid line*) and for a nearly symmetric cavity having the same cavity length

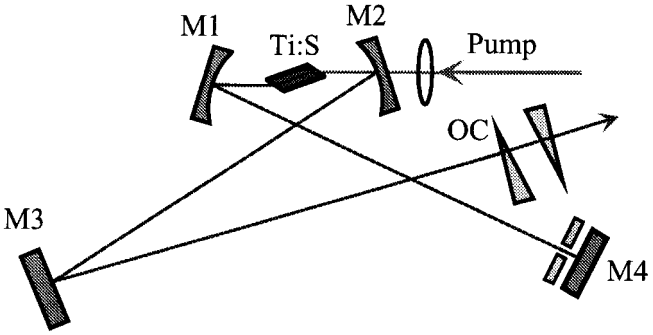

Fig. 5. Schematic diagram of the MDC Ti:sapphire oscillator used for soft-aperture and hard-aperture mode locking. M1–M4, broadband chirped mirrors exhibiting high reflectivity over the wavelength range of 650 to 950nm and a nearly constant negative GDD over the range of 690 to 900nm; OC, output coupler deposited on a thin wedged fused-silica substrate (for transmittivity, see the text). The wedged compensation plate placed outside the laser cavity is used for compensating the angle dispersion introduced by the wedged substrate of the output coupler OC

zone (corresponding to the larger separation between the focusing mirrors) [32]. The importance of an asymmetric cavity was also verified experimentally [33, 34]. According to previous studies [33, 34] and our experience, the range of values of the asymmetry parameter γ quoted above for hard-aperture KLM systems seems to yield optimum performance also for the case of soft aperture mode locking.

The layout of the MDC-KLM Ti:sapphire oscillator we have developed for the generation of sub-10-fs pulses is shown in Fig. 5. The resonator is formed by four chirped mirrors M1–M4 and an output coupler OC. The four chirped mirrors introduce a negative group delay dispersion of $\approx -340\,\text{fs}^2$, which, aside from some fluctuations inherent to broadband chirped mirrors made up of discrete layers [13], is approximately constant all the way from 690 to 900 nm. Moreover, the mirrors exhibit negative GDD down to wavelengths as short as 660 nm, allowing the mode-locked spectrum to extend well below 700 nm for the first time. Details about the chirped mirrors with improved characteristics will be published elsewhere [22]. The lengths of the cavity arms confined by M1–M4 and M2–OC have been set equal to $d_1 \approx 118\,\text{cm}$ and $d_2 \approx 68\,\text{cm}$ as a result of the considerations discussed above. The two curved mirrors have a radius of curvature of 50 mm. The chirped mirrors deposited on the curved substrates have a transmittivity of higher than 90% in the wavelength range of 485–535 nm, permitting the use of either an argon laser or a frequency-doubled neodymium laser as a pump source. The path length of the resonator mode through the heavily doped Ti:S crystal slab inserted at Brewster's angle is 2.3 mm. The absorption coefficient of the doped Xtal is $5\,\text{cm}^{-1}$ at 514 nm, implying a pump absorption efficiency of $\approx 70\%$.

In this cavity design the confocal parameter of the resonator mode in the gain medium is comparable to the 2.3-mm path length in the crystal, i.e. the effective mode cross-sectional area in the gain medium has been chosen to minimize the pumping threshold rather than compromizing it for an increased mode-locked pulse energy extractable corresponding to requirement (i) in the previous section. This is because up to a pump power level of $\approx 5\,\text{W}$, successful implementation of options (ii) and (iii) (see previous section) has proved sufficient for achieving good energy extraction

in mode-locked operation. Absorbed pump powers at around 5 W are of particular interest because of the recent availability of commercial all-solid-state (diode-pumped) pump sources in this power range. Optimization of the KLM performance for significantly higher absorbed pump powers, however, may require expansion of the mode diameter in the Xtal according to (i).

In an attempt to partially compensate for the increased pumping threshold due to an increased output coupling according to (iii), we have focused the pump beam more tightly by shortening the focal length of the pump focusing lens from its previously used value of 40 mm [14, 15] to 30 mm and developed a new cooling system. Whereas the effective pump beam cross-sectional area explicitly affects the pumping threshold [35], the crystal temperature has an indirect influence; the upper-state lifetime of the laser transition in Ti:S rapidly decreases as the crystal temperature considerably exceeds room temperature [36]. This had been the case in all Ti:S lasers (including those commercially available) until recently. Excessive temperature in the pumped volume results in a reduction of the upper-state lifetime and thereby an enhanced threshold [35] and reduced output power. To improve the situation, we have developed a new cooling configuration in which one transverse dimension of the tiny Ti:S slab is as small as 1 mm or less, permitting the Xtal to be sandwiched transversally in spite of its small longitudinal extension (separation of the polished surfaces ≈ 2.1 mm). As a result, the heat sink (cooled by a Peltier cooler) is brought in close proximity to the pumped volume, providing extremely efficient heat removal. The new cooling system (patent pending) has proved a key innovation which allows efficient operation of a Ti:S laser using output coupling well in excess of 10% at absorbed pump-power levels as low as 3–5 W for what is to our knowledge the first time. High output coupling, on the other hand, is a prerequisite for megawatt-scale peak powers from a cw mode-locked laser.

The other indispensable requirement for the generation of pulses with high peak powers from a laser oscillator is the presence of efficient SAM action in the cavity. This can be accomplished by the introduction of a semiconductor saturable absorber [37], which is able to introduce a strong SAM in addition to that created by KLM. Alternatively, the interplay between self-focusing (in the gain medium) and an intracavity aperture can be optimized to yield maximum discrimination of low-power radiation against high-power radiation. In our attempts to achieve the highest possible peak power from sub-10-fsTi:sapphire oscillators, we have opted for the latter approach, because the unavoidable insertion loss introduced by any additional intracavity component tends to interfere with the above objective.

KLM using a hard aperture has been optimized by drawing on the theoretical results of Brabec et al. [6, 38]. The aperture is introduced at M4, the mirror terminating the shorter collimated arm, and δ is adjusted to be close to δ_1 in the first stability zone (see Fig. 3). This stability zone was chosen because of the convenience related to a larger mode spot size at the position of the aperture as compared with the other option represented by $\delta \rightarrow \delta_2$ (see Fig. 2). In addition to the change in the beam profile due to a direct consequence of self-focusing [3], which results in the SAM-coefficient depicted in Figs. 3 and 4, a strong indirect effect has also been exploited, namely a longitudinal shift of the beam waist along the cavity axis, which was predicted to introduce a strong change in the beam diameter at the cavity ends under certain conditions [38]. For this effect to be efficiently utilized, the folding angles at M1 and M2 *must be different*. Experimentally, a ratio of $\alpha_1/\alpha_2 \approx 2/3$ has been found to provide the maximum SAM effect without degradation of the output beam quality, where α_1 and α_2 represent the (full) folding angles at mirrors M1 and M2. The values of the folding angles are determined by the requirement of compensating the astigmatism introduced by the Brewster-angled gain medium by that of the curved mirrors used at an oblique incidence [39]. This requirement along with the above quoted ratio of α_1 to α_2 yields $\alpha_1 = 12^\circ$ and $\alpha_1 = 18^\circ$ for our cavity parameters.

The depth of SAM could be further enhanced by replacing the widely used vertical slit [3] with an adjustable elliptical aperture with its longer axis aligned vertically. The length of the vertical axis has been matched with the vertical beam size such that the aperture does not clip the beam along this direction, along which the beam is subjected to relatively small KLM-induced changes [38]. The shorter horizontal axis of the aperture is adjusted to introduce a linear insertion loss, which is reduced due to self-focusing. As compared with the previously used vertical slit, the elliptical aperture provides a better discrimination in favor of the mode-locked state because its shape follows more closely the KLM-induced change in the beam profile (patent pending).

When implementing KLM by exploiting the aperturing action of the cylindrical pumped volume in the gain medium, the same resonator configuration as for hard-aperture KLM is used, except that the hard aperture is removed and the separation of the curved mirrors M1 and M2 is increased to shift the stability parameter close to δ_2 in the second stability zone, as suggested by the theoretical work of Piché and Salin [32]. An asymmetry of the folding angles similar to that quoted above for hard-aperture KLM has been found to be helpful but not indispensable; stable soft-aperture mode locking in the sub-10-fs regime could also be obtained with $\alpha_1 \approx \alpha_2$. However, our experiments have revealed that the sum of the two folding angles is a critical parameter for soft-aperture KLM (at least in a sub-10-fs oscillator). Optimum performance of soft-aperture KLM (in terms of pulse energy and pulse duration) has been found to rely upon a value of $\alpha_1 + \alpha_2$ that is by a few degrees larger than that required for proper astigmatic compensation as given by [39]. As a result, the output of a sub-10-fs Ti:S laser mode-locked by soft-aperture KLM optimized for minimum pulse width and maximum pulse energy tends to be delivered in a somewhat asymmetric and astigmatic beam (see below).

Owing to the careful optimization of the resonator parameters for best KLM performance, SAM introduced by either of the two aperturing mechanisms is sufficiently strong sufficiently far (a few tens of micrometres) away from the boundaries δ_1 or δ_2 of the stability zones that mode locking can be kept stable for unlimited periods without the need for cavity realignment. In the systems described in more detail in the following section we estimate the change in the round-trip gain induced by the peak of the mode-locked pulse as $\Delta g_{\text{peak}} \approx 0.04 - 0.06$. Although the systems are not self-starting, once optimized, simply tapping one of the cavity mirrors starts mode locking, which has been found to be quite robust against various kinds of environmental perturba-

tions. Carefully designed commercial versions of the systems presented here have been found to be fully operational in a number of various environments outside optical laboratories.

3 Characteristics of sub-10 fs MDC Ti:S oscillators pumped by an argon laser

In this section we shall characterize the above-described MDC Ti:S oscillators pumped by the blue-green lines of a small-frame argon laser (Innova 310, Coherent) in terms of the most important laser parameters, such as pulse energy, mode-locked spectral width, pulse duration, pulse energy fluctuations, timing jitter, and beam quality. The absorbed pump power has been kept constant at ≈ 5.5 W in all the experiments described in this section. The results presented below have been obtained with the same oscillator first optimized for hard-aperture KLM and subsequently for soft-aperture KLM, allowing a direct comparison of the performances of the two different SAM mechanisms in the sub-10-fs time domain.

3.1 Pulse energy, duration, and spectral width.

Other than the efficiency of the KLM, the output coupling has been found to be a key parameter for the realization of maximum output pulse energy at the shortest possible pulse durations. The maximum output coupling permitting stable mode-locked operation using hard-aperture KLM has been found to be $\approx 16\%$ at the pump power level given above. By contrast, stable mode locking up to an output coupling as high as $\approx 23\%$ has been obtained by soft-aperture KLM. Considering that the hard aperture introduces an estimated double-pass small-signal loss of $6-8\%$ we may conclude that both systems tolerate a round-trip cavity loss of around 25% at an absorbed pump power of 5–6 W. With the 16% output coupler used in combination with the hard aperture and the 23% output coupler employed in the soft-aperture system, the mode-locked oscillator delivers an average output power of 620 and 720 mW at a pulse repetition rate of 77 MHz, respectively. This results in an output pulse energy of 8.1 and 9.4 nJ for the systems mode-locked by using a hard and a soft aperture, respectively. The intracavity pulse energy is around 50 nJ or slightly less. Attempts to increase the mode-locked output power by increasing the pump power have resulted in multiple pulsing or the emergence of a cw background, in agreement with previous observations [10].

The spectrum and the interferometric autocorrelation of the output obtained from the hard-aperture system are shown in Figs. 6 and 7, respectively. Dispersion compensation outside the cavity has been accomplished by realizing four reflections off chirped mirrors, and the net extracavity GDD is set equal to zero by translating the wedged compensation plate shown in Fig. 5. The dashed lines in Fig. 7 depict the envelopes of the interferometric autocorrelation of a 7.5-fs pulse having a $sech^2$ temporal intensity profile. The autocorrelator had been calibrated with an He−Ne laser. Fourier-transform of the spectrum shown in Fig. 6, which is not corrected for the response of the spectrometer and the silicon photodiode used, yields a pulse duration slightly below 7.5 fs. The actual transform-limited pulse duration is likely to be somewhat

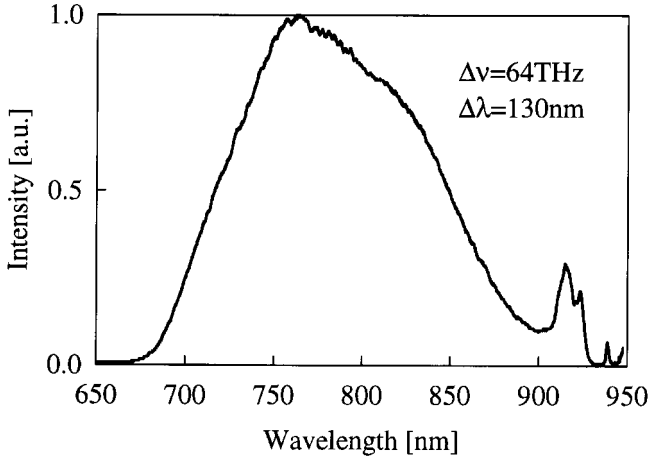

Fig. 6. Spectrum of the MDC Ti:S oscillator Kerr-lens mode-locked using a hard aperture

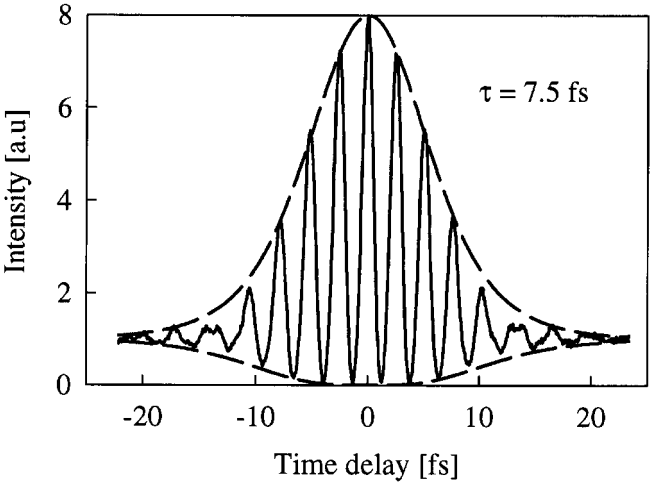

Fig. 7. Fringe-resolved (interferometric) autocorrelation trace of the output of the MDC Ti:S oscillator mode locked using a hard aperture

shorter because correction of the measured spectrum for the wavelength dependence of the detector response and the grating efficiency (which is not known) is expected to slightly broaden the spectrum. Given the uncertainty in the spectral intensity and the unknown spectral phase, we estimate the pulse duration to be 7.5 ± 0.5 fs. Using the soft aperture in KLM produces mode-locked spectra that are up to 10% broader than that shown in Fig. 6. However, no appreciable change in the autocorrelation trace as compared with Fig. 7 has been found. This observation supports the hypothesis that uncompensated third-order dispersion inside and outside the resonator limits the pulse duration to 7–8 fs.

Owing to the combination of extremely short pulse durations and relatively high pulse energies, the presented MDC systems generate pulses with peak powers in excess of 1 MW, a value that could not be demonstrated previously by any other cw mode-locked laser. To demonstrate the usefulness of this unprecedented performance, we have performed frequency doubling of this output in a 300-μm-thick LBO crystal cut for Brewster incidence. The fundamental beam having a diameter of ≈ 2 mm has been focused by a spherical mirror of a radius of curvature of 25 mm onto the LBO crystal. With this

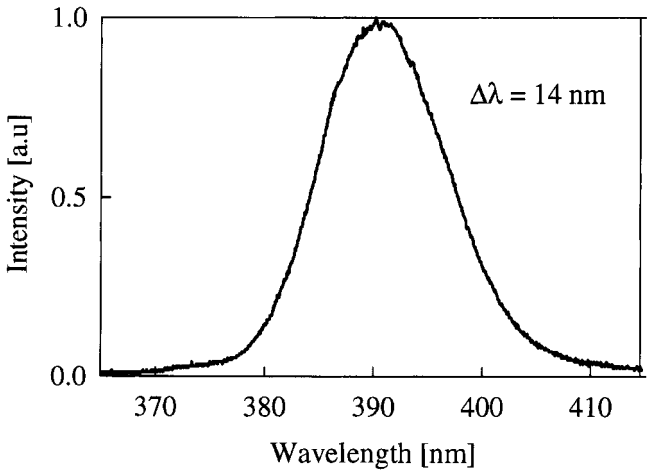

Fig. 8. Spectrum of the frequency-doubled output of the 1-MW sub-10-fs MDC Ti:S laser. See the text for details of the experiment

simple setup we have produced 120 mW of femtosecond blue light by using ≈ 600 mW of the output from the hard-aperture system, implying a conversion efficiency of 20%. The spectrum of the frequency-doubled output is shown in Fig. 8. The 14-nm bandwidth should allow the generation of sub-15-fs pulses at ≈ 390 nm. This combination of short pulse duration and high average power is unprecedented in the blue spectral range [40, 41]. We expect that employing diffraction-limited f/2 focusing optics in combination with a thinner frequency-doubling crystal will allow the generation of sub-10-fs blue pulses at average power levels in excess of 200 mW by using a megawatt-scale sub-10-fs Ti:sapphire oscillator.

3.2 Pulse energy fluctuations, timing jitter.

The pulse parameters in the output pulse train delivered by a sub-10-fs oscillator are, just as in any mode-locked laser, subject to fluctuations. Deviations from the ideal case of a periodic train of identical pulses manifest themselves, among other ways, in fluctuations of the pulse energy and of the time of their appearance at some fixed position outside the cavity (timing jitter). As first proposed by von der Linde [42], pulse energy noise and timing jitter can be evaluated from measurements of the radiofrequency (RF) power spectrum of the mode-locked laser output. Drawing on the approach of von der Linde we have performed a comprehensive noise characterization of our sub-10-fs oscillators [43]. Here we present a brief summary of the results most important for practical applications.

Figure 9a shows the energy noise spectral density of the sub-10-fs Ti:sapphire oscillators along with the power noise spectrum of the argon laser used as a pump source. The pulse energy fluctuations of both sub-10-fs systems originate entirely from the noise of the pump source for frequencies higher than 300 Hz. The increased pulse energy noise with respect to the pump noise for $f < 300$ Hz is assumed to arise from environmental perturbations, including vibrations of the mechanical components of the resonator and possible air turbulances. The timing jitter of the same systems under the same operating conditions is shown in Fig. 9b. The increased spectral density of the hard-aperture system at around 100 Hz

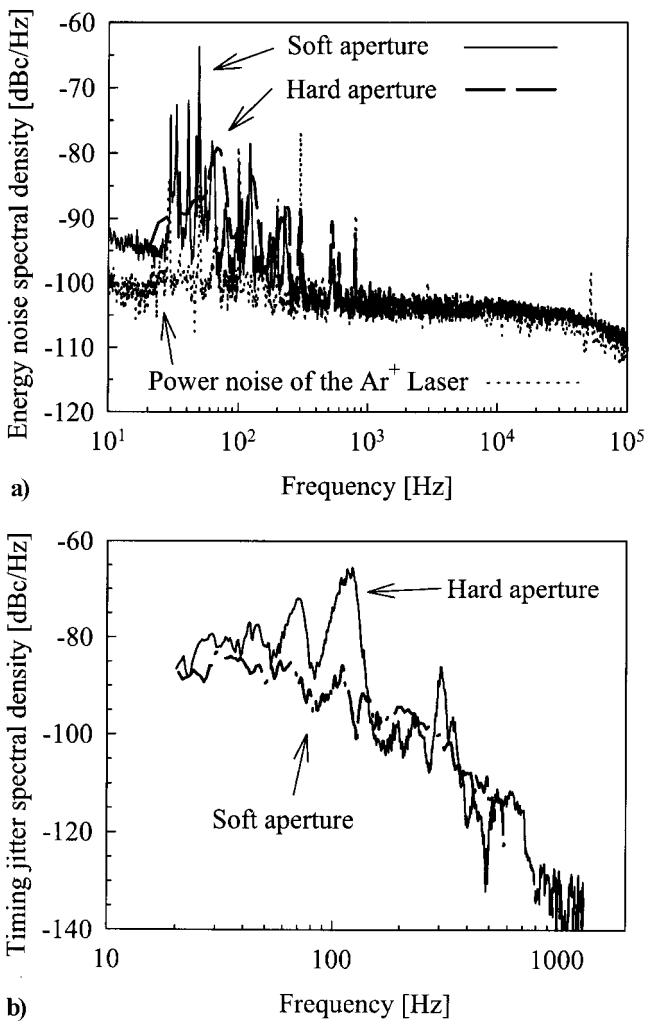

Fig. 9a,b. Radio-frequency spectrum of the energy noise (**a**) and timing jitter (**b**) of sub-10-fs MDC-KLM Ti:S oscillators pumped by an argon laser

correlates with similar features in the energy noise spectrum, indicating a coupling between energy noise and timing jitter. The root mean square (RMS) of the energy noise and tim-

Table 1. Integrated RMS energy noise and timing jitter for sub-10-fs MDC Ti:S oscillators Kerr-lens mode-locked by using hard and soft apertures and pumped by an argon laser

Integrated RMS energy noise (%)		
Range (Hz)	Hard aperture	Soft aperture
2 – 20	–	0.017
20 –200	0.086	0.101
200 – 2 k	0.063	0.045
2 k– 20 k	0.126	0.114
20 k–100 k	0.187	0.194
100 k– 2 M	0.138	–
20 –100 k	**0.249**	**0.251**
Integrated RMS timing jitter (ps)		
Range (Hz)	Hard aperture	Soft aperture
20– 200	6.53	1.42
200–2000	< 0.66	< 0.46
20–2000	**6.56**	**1.49**

ing jitter integrated over different spectral regions are listed in Table 1. The measured RMS energy noise, well below 1% in the frequency range where appreciable fluctuations arise, provides clear evidence for the stability and robustness of these sub-10-fs oscillators.

3.3 Beam quality.

The peak intensity of the generated pulses that can be achieved by focusing is important for many applications where nonlinear effects are investigated or exploited. It depends on the peak power and the extent to which the laser beam delivering the pulses is diffraction-limited. In order to quantify this extent we investigated the evolution of the transverse intensity distribution during propagation. To this end, the laser was gently focused by a low F-number optics. The beam profile was then measured by a CCD (Charge Coupled Device) matrix detector. The transverse intensity distribution was Gaussian,

$$I(x, y, z) = I_0 \exp\left(-\frac{2x^2}{w_x^2(z)} - \frac{2y^2}{w_y^2(z)}\right) \tag{4}$$

with spot sizes given by

$$w_x^2(z) = w_{x0}^2 + M_x^4 \times \frac{\lambda^2}{\pi^2 w_{x0}^2}(z - z_{0x})^2 \tag{5}$$

and

$$w_y^2(z) = w_{y0}^2 + M_y^4 \times \frac{\lambda^2}{\pi^2 w_{y0}^2}(z - z_{0y})^2 \tag{6}$$

in all cases to a good accuracy. The factors M_x^2 and M_y^2, which are equal or greater than 1, are a measure of the far field spot size of the beam relative to that of an ideal diffraction-limited Gaussian beam with the same beam waist, w_{x0} and w_{y0}, respectively [44]. The measured spot sizes in the tangential and sagittal planes, or horizontal and vertical directions, respectively, are shown in Fig. 10. The output of the high-power sub-10-fs laser mode-locked by using a hard aperture can be focused to a circular spot in the focal plane as shown by Fig. 10a. Consequently, the beam is symmetric ($w_{x0} = w_{y0}$) and is free from astigmatism ($z_{0x} = z_{0y}$). However, the M^2 parameter is found to be different for the tangential (x) and sagittal (y) planes. From the fits represented by the solid and dashed lines in Fig. 10a we have evaluated $M_x^2 = 1.02$ and $M_y^2 = 1.33$. By contrast, the laser beam delivered by the soft-aperture KLM system optimized for maximum output pulse energy is found to be both asymmetric ($w_{x0} \neq w_{y0}$) and astigmatic ($z_{0x} \neq z_{0y}$), as shown in Fig. 10b. We anticipate that the latter can be compensated by some astigmatic telescopic system outside the cavity. Fitting again Eqs. (5) and (6) the measured variation of the corresponding spot sizes represented by the full and open circles in Fig. 10b yields the solid and dashed lines, respectively. From this analysis we have inferred $M_x^2 = 1.05$ and $M_y^2 = 1.45$. It is interesting to notice that in both systems the laser beam exhibits a nearly perfect spatial coherence in the tangential plane, whereas it is slightly degraded in the sagittal plane. We conjecture that the better mode quality in the horizontal plane might relate to the stronger nonlinear spatial filtering action taking place in this plane.

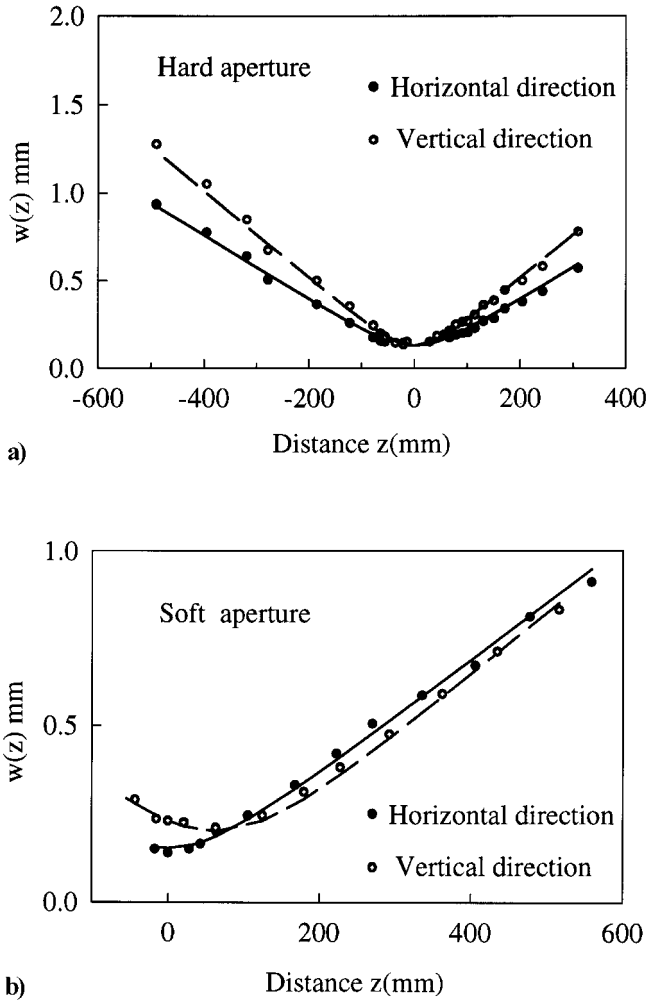

Fig. 10a,b. Gaussian-beam spot size versus propagation distance around the focal region of a low F-number focusing lens in the horizontal and vertical direction for KLM accomplished by using a hard aperture (**a**) and the soft (gain) aperture (**b**) in the sub-10-fs Ti:S oscillator optimized for maximum output pulse energy. Full and open circles, measured data; solid and dashed lines, calculated spot size using (5) and (6) with M_x^2 and M_y^2 as fit parameters, respectively

4 All-solid-state sub-10-fs Ti:S oscillator

Recently, diode-pumped continuous-wave intracavity-frequency-doubled neodymium lasers specified for 5-W output power at $\lambda = 0.53\,\mu$m have been developed by two manufacturers, Spectra Physics and Coherent. The systems offered by both of these manufacturers are ideally suited as pump sources for the Ti:S oscillators described above. Recently, we have demonstrated highly stable and reliable operation of a sub-10-fs Ti:S oscillator pumped by a 5-W diode-pumped green laser (Millennia, Spectra Physics) [43]. Using the hard-aperture KLM system described above, pulses of durations of 8–9 fs at an average power of ≈ 400 mW can be generated when the laser is pumped by 5 W of the Millennia output. This implies an absorbed pump power of ≈ 3 W.

The corresponding pulse energy of > 5 nJ together with the sub-10-fs pulse duration results in a peak power higher than 0.5 MW. Owing to the more stable output of the diode-pumped neodymium laser as compared with the argon laser, the all-solid-state sub-10-fs Ti:S oscillator exhibits a significantly lower energy noise in the frequency range of 1 to 200 kHz than its argon-laser-pumped counterpart (Fig. 11a). The all-solid-state system also performs better with respect to timing jitter (Fig. 11b), which also supports the hypothesis regarding the presence of some mechanism giving rise to a coupling between energy fluctuations and timing jitter.

We expect that the output power of the all-solid-state sub-10-fs laser can be significantly increased by retroreflecting the residual (transmitted) pump beam into the gain medium and/or employing a more heavily doped crystal. These improvements hold out the promise of producing 1-MW sub-10-fs pulses from an all-solid-state Ti:sapphire laser. This performance together with the excellent noise characteristics and the solid-state reliability makes the present system attractive for many applications in science, technology, and medicine.

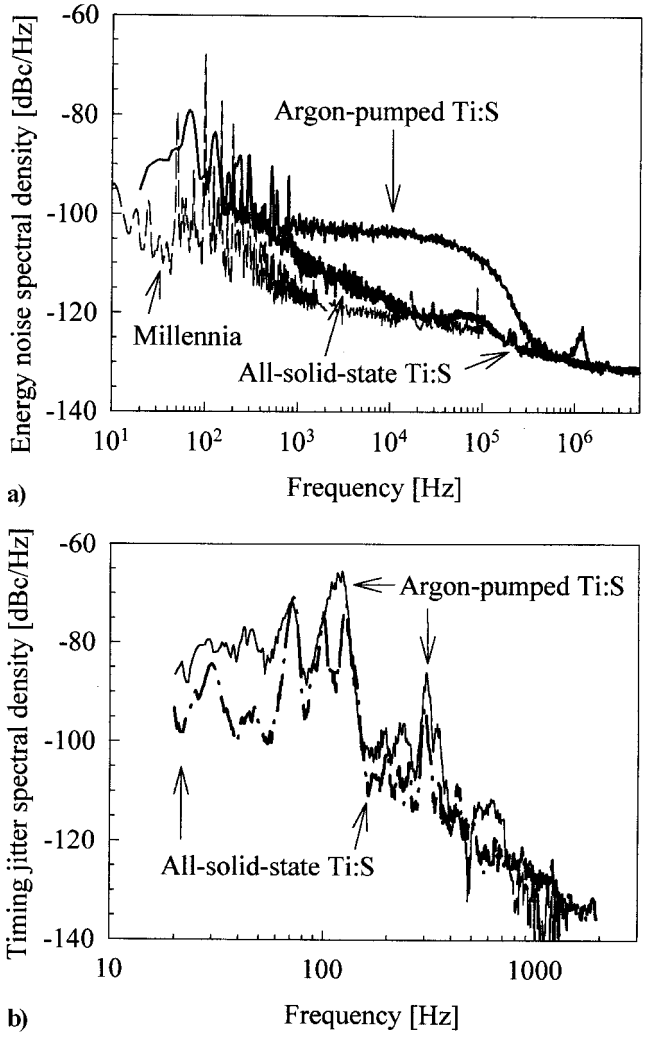

Fig. 11a,b. Radio-frequency spectrum of the energy noise (**a**) and timing jitter (**b**) of sub-10-fs MDC Ti:S oscillators Kerr-lens mode-locked by using a hard aperture and pumped by an argon laser or a frequency-doubled diode-pumped neodymium laser (Millenia, Spectra-Physics Inc.)

Acknowledgements. We wish to thank A.J. Schmidt for his support and Spectra Physics for the generous loan of the diode-pumped neodymium laser (Millennia). This research has been sponsored by the Fonds zur Förderung der wissenschaftlichen Forschung grants P9710 and P10409, and by the Österreichische Nationalbank grants 5335 and 5124.

References

1. P.F. Moulton: J. Opt. Soc. Am. B **3**, 125 (1986)
2. D.E. Spence, P.N. Kean, W. Sibbett: Opt. Lett. **16**, 42 (1991)
3. L. Spinelli, B. Couillaud, N. Goldblatt, D.K. Negus: In *Digest of Conference on Lasers and Electro-Optics* (Optical Society of America, Washington, D. C., 1991), Paper CPDP7
4. U. Keller, G.W. tHooft, W.H. Knox, J.E. Cunningham: Opt. Lett. **16**, 1022 (1991)
5. M. Piché, Opt. Commun. **86**, 156 (1991)
6. T. Brabec, Ch. Spielmann, P.F. Curley, F. Krausz: Opt. Lett. **17**, 1292 (1992)
7. H.A. Haus, J.G. Fujimoto, E.P. Ippen: J. QE-**28**, 2086 (1992)
8. C.P. Huang, H.C. Kapteyn, J.W. McIntosh, M.M. Murnane: Opt. Lett. **17**, 139 (1992); F. Krausz, C. Spielmann, T. Brabec, E. Wintner, A.J. Schmidt: Opt. Lett. **17**, 204 (1992); C.P. Huang, M.T. Asaki, S. Backus, M.M. Murnane, H.C. Kapteyn, H. Nathel: Opt. Lett. **17**, 1289 (1992); B. Proctor, F. Wise: Opt. Lett. **17**, 1295 (1992); B.E. Lemoff, C.P.J. Barty: Opt. Lett. **17**, 1367 (1992)
9. Ch. Spielmann, P.F. Curley, T. Brabec, E. Wintner, F. Krausz: Electron. Lett. **28**, 1532 (1992); P.F. Curley, Ch. Spielmann, T. Brabec, F. Krausz, E. Wintner, A.J. Schmidt: Opt. Lett. **18**, 54 (1993); B. Proctor, F. Wise: Appl. Phys. Lett. **62**, 470 (1993); M. Asaki, C. Huang, D. Garvey, J. Zhou, H.C. Kapteyn, M.M. Murnane: Opt. Lett. **18**, 977 (1993)
10. Ch. Spielmann, P.F. Curley, T. Brabec, F. Krausz: J. QE-**30**, 1100 (1994)
11. J. Zhou, G. Taft, C.P. Huang, M.M. Murnane, H.C. Kapteyn, I. Christov: Opt. Lett. **19**, 1149 (1994)
12. I.P. Christov, M.M. Murnane, H.C. Kapteyn, J.P. Zhou, C.P. Huang: Opt. Lett. **19**, 1465 (1994)
13. R. Szipöcs, K. Ferencz, Ch. Spielmann, F. Krausz: Opt. Lett. **19**, 201 (1994); see also the article of R. Szipöcs to be published in this same issue
14. A. Stingl, Ch. Spielmann, F. Krausz, R. Szipöcs: Opt. Lett. **19**, 204 (1994)
15. A. Stingl, M. Lenzner, Ch. Spielmann, F. Krausz, R. Szipöcs: Opt. Lett. **20**, 602 (1995)
16. A. Kasper and K. J. Witte, Opt. Lett. **21**, 360 (1996)
17. L. Xu, Ch. Spielmann, F. Krausz, R. Szipöcs: Opt. Lett. **21**, 1259 (1996)
18. T. Brabec, Ch. Spielmann, F. Krausz: Opt. Lett. **16**, 1961 (1991)
19. M. Ramaswamy, M. Ulman, J. Paye, J.G. Fujimoto: Opt. Lett. **18**, 1822 (1993)
20. M.S. Pshenichnikov, W.P. de Boeij, D.A. Wiersma: Opt. Lett. **19**, 572 (1994)
21. See, for instance, the relevant contributions in this issue
22. G. Tempea, Ch. Spielmann, F. Krausz, K. Ferencz: unpublished
23. E.P. Ippen: Appl. Phys. B. **58**, 159 (1994)
24. H.A. Haus: In *Compact Sources of Ultrashort Pulses*, ed. by I.N. Duling, III, (Cambridge University Press, Cambridge 1995) p. 1
25. T. Brabec, S.M.J. Kelly, F. Krausz: In *Compact Sources of Ultrashort Pulses*, ed. by I.N. Duling, III, (Cambridge University Press, Cambridge 1995) p. 57
26. F.X. Kärtner, D. Kopf, U. Keller: J. Opt. Soc. Am. B **12**, 486 (1995)
27. H. Kogelnik: Bell. Syst. Tech. J. **44**, 455 (1965)
28. A.E. Siegman: *Lasers* (University Science Books, Mill Valley, CA, 1986)
29. J.H. Marburger: Prog. Quantum Electron. **4**, 35 (1975)
30. D. Huang, M. Ulman, L.H. Acioli, H.A. Haus, J.G. Fujimoto: Opt. Lett. **17**, 511 (1992)
31. G. Cerullo, S. De Silvestri, V. Magni: Opt. Lett. **19**, 1040 (1994)
32. M. Piche, F. Salin: Opt. Lett. **18**, 1041 (1993)

33. M. Asaki, C. Huang, D. Garvey, J. Zhou, H.C. Kapteyn, M.M. Murnane: Opt. Lett. **18**, 977 (1993)
34. K. Read, F. Blonigen, N. Ricelli, M. Murnane, H. Kapteyn: Opt. Lett. **21**, 489 (1996)
35. F. Krausz, E. Wintner, A.J. Schmidt, A. Dienes: J. QE-**26**, 158 (1990)
36. P. Albers, E. Stark, G. Huber: J. Opt. Soc. Am. B **3**, 134 (1986)
37. U. Keller: Appl. Phys. B **58**, 347 (1994), see also contributions from the same group to this issue.
38. T. Brabec, P.F. Curley, Ch. Spielmann, E. Wintner, A.J. Schmidt: J. Opt. Soc. Am. B **10**, 1029 (1993)
39. H.W. Kogelnik, E.P. Ippen, A. Dienes, C. V. Shank: J. QE-**8**, 373 (1972)
40. S. Backus, M.T. Asaki, C. Shi, H.C. Kapteyn, M.M. Murnane: Opt. Lett. **19**, 399 (1994); M.T. Asaki, S. Backus, C. Baldwin, C. Shi, M.M. Murnane, H.C. Kapteyn: In *Ultrafast Phenomena IX*, ed. by P.F. Barbara, W.H. Knox, G.A. Mourou, A.H. Zewail: (Springer, 1994) p. 213
41. S.H. Ashworth, M. Joschko, M. Woerner, E. Riedle, T. Elsaesser: Opt. Lett. **20**, 2120 (1995)
42. D. von der Linde, Appl. Phys. B **39**, 201 (1986)
43. A. Poppe, L. Xu, A. Stingl, Ch. Spielmann, F. Krausz: “Noise characterization of sub-10 fs Ti:sapphire oscillators” (unpublished)
44. A.E. Siegman: in *SPIE Proceedings Series Optical Resonators* Vol. 1224 (The Society, Bellingham, WA 1990) p. 2